Static universality class for gadolinium

S. Srinath and S. N. Kaul*
School of Physics, University of Hyderabad, Central University P.O., Hyderabad 500 046, Andhra Pradesh, India
(Received 6 April 1999)

High-precision magnetization, $M(T,H)$, data have been taken along the c axis (easy direction of magnetization) of a high-purity Gd single crystal in the critical region near the ferromagnetic-paramagnetic phase transition. Elaborate data analyses demonstrate that the single power laws, by themselves, do not adequately describe the observed field dependence of M at the Curie point T_C, $M(T_C,H)$, and the temperature variations of spontaneous magnetization, $M(T,0)$, and initial susceptibility, $\chi(T)$, in the asymptotic critical region $|\epsilon| = |(T-T_C)/T_C| \leqslant 2\times 10^{-3}$, but do so only when the multiplicative logarithmic corrections (LC), predicted by the renormalization group (RG) calculations for dipolar Ising (spin dimensionality $n=1$) spin systems at the upper marginal space dimension $d^*=3$, are taken into account. Such data analyses also permit the first accurate determination of LC exponents (x',x), the asymptotic critical exponents β, γ, and δ, and critical amplitudes $\hat{B}$, $\hat{\Gamma}$, and $\hat{D}$ for $M(T,0)$, $\chi(T)$, and $M(T_C,H)$. The exponents x', x, β, γ, and δ, as well as the universal amplitude ratio $R_\chi = \hat{D}\hat{B}^{\delta-1}\hat{\Gamma}$ possess the *same* (within the uncertainty limits) values as those yielded by the RG calculations for a $d=3$ uniaxial dipolar ferromagnet. Moreover, the presently determined values of β, γ, and δ, together with the reported value of the specific heat critical exponent α, obey the scaling relations $\beta+\gamma=\beta\delta$ and $\alpha+2\beta+\gamma=2$ accurately. By establishing that gadolinium belongs to the $d=3$, $n=1$ *dipolar* static universality class, the present results resolve the long-standing controversy surrounding the nature of the asymptotic critical behavior of Gd. [S0163-1829(99)11941-6]

I. INTRODUCTION

The practice of assigning a universality class, specified by the *lattice* dimensionality ''d'' and *order parameter* dimensionality ''n,'' to a given system based on the values of critical exponents that characterize its asymptotic critical behavior, has facilitated the understanding of critical phenomena in several materials in the past. However, an unambiguous identification of a real system with any one of the known universality classes has not been always possible. One such exception to the general rule (which is the main concern of this paper) is gadolinium metal. The relevant details of this case are furnished below. Considering that gadolinium metal is made up of *spherically symmetric* $^8S_{7/2}$ Gd^{3+} ions and *isotropic* Ruderman-Kittel-Kasuya-Yosida (RKKY) interactions between *localized* $4f$ magnetic moments give rise to ferromagnetism in this metal, gadolinium is expected to exhibit extremely *weak* magnetocrystalline anisotropy and behave as an *isotropic* three-dimensional *Heisenberg* ferromagnet in the critical region. Hence, gadolinium should figure among the systems that form the $d=3$, $n=3$ universality class. Contrary to this expectation, overwhelming experimental evidence[1–9] in favor of a small *uniaxial* anisotropy, which ensures that the c axis of the hexagonal-close-packed (hcp) lattice is the preferred orientation of magnetization in gadolinium at temperatures $\gtrsim 240$ K that embrace the critical region, asserts that the critical behavior of gadolinium is that of a three-dimensional *Ising* ferromagnet. Thus, gadolinium should fall within the $d=3$, $n=1$ universality class.

Existence of uniaxial[1–9] magnetic ordering at temperatures in the vicinity of Curie point, T_C, is inconceivable within the framework of the conventional theories of magnetocrystalline anisotropy, but the theory due to Fujiki, De'Bell, and Geldart[10] offers the following explanation for this observation. According to this theory, the long-range dipole-dipole interactions between magnetic moments localized at the sites of the hcp lattice *favor* the c axis as the *easy* direction of magnetization when the unit-cell parameter ratio c/a falls *below* its *ideal* value of $c/a \simeq 1.63$. In the case of gadolinium, the c/a ratio assumes the value 1.59 for temperatures in the close proximity to T_C. This viewpoint is further strengthened by the fact that the *characteristic* temperature scale for *uniaxial* anisotropy, estimated from magnetic susceptibility data[11] taken along the c axis and in the basal plane on a single crystal of Gd in the critical region, is completely accounted for[11,12] by the dipole-dipole interactions. Early renormalization group (RG) calculations revealed that dipolar interactions change only *slightly*[13–15] the critical exponents of the $d=n=3$ system but *drastically* modify[16–19] the critical behavior of the $d=3$, $n=1$ system so much so that the system exhibits *mean-field* behavior with *logarithmic* corrections[16–19] in the asymptotic critical region; this behavior is *characteristic* of *uniaxial dipolar* ferromagnets.[20–23] In view of this RG result, dipolar interactions, which are responsible for uniaxial magnetic ordering in Gd at temperatures close to, and around, T_C are expected to have a decisive influence on its asymptotic critical behavior. RG treatment[18,19] of spin systems, such as Gd, in which *uniaxial* dipolar (UD) and *isotropic* dipolar (ID) interactions of normalized coupling strengths g_{UD} and g_{ID} (such that $g_{UD} \ll g_{ID}$) occur in association with isotropic Heisenberg interactions predicts the sequence of crossovers: Gaussian regime $\rightarrow$ isotropic short-range Heisenberg $\rightarrow$ isotropic dipolar $\rightarrow$ uniaxial dipolar fixed point when temperature is lowered from high temperatures to T_C.

During the past three decades, numerous experimental at-

tempts have been made to study static critical behavior of Gd near the ferromagnetic (FM) -to - paramagnetic (PM) phase transition. Critical exponents $\alpha^{\pm}$ (plus and minus signs refer to temperatures above and below T_C), β, γ, and δ for specific heat, $C(T,H=0)$, spontaneous magnetization, $M(T,H=0)$, magnetic susceptibility, $\chi(T)$, and M vs H *critical* isotherm (at $T=T_C$), respectively, have been determined from the measurements of specific heat,[24–27] thermal expansion,[26,28] electrical resistivity,[29] $\rho(T,H=0)$, magnetization,[30–37] perturbed angular correlation[38] and magnetic susceptibility.[39–42] The most reliable values of the critical exponents $\alpha^{\pm}$, β, γ, and δ published prior to 1990 have been compiled in Refs. 36–39 and 43. Early determinations[26,28] of $\alpha^{\pm}$ yielded *anomalously large* values whose sign happens to agree with that predicted by the three-dimensional Heisenberg model.[44] Subsequent investigations[27,29] not only corrected such unphysically large exponent values but also demonstrated that in the reduced temperature range $1.5\times10^{-4}\lesssim|\epsilon|=|T-T_C|/T_C\lesssim 1.0\times10^{-3}$, the $\rho(T,H=0)$ and $C(T,H=0)$ data are consistent with the mean-field behavior (i.e., $\alpha^{\pm}=0$) with logarithmic corrections. As far as the reported values of the remaining critical exponents are concerned, the numerical estimates for β and γ, obtained in the reduced temperature range $|\epsilon|>10^{-3}$, cluster around[30–41,43] 0.39 and 1.24, respectively, whereas those of δ range between[30–37] 3.6 and 4.4. While the value $\beta\simeq0.39$ suggests that Gd belongs to the $d=n=3$ universality class,[44] $\gamma\simeq1.24$ indicates that the critical behavior of Gd is that of a $d=3$ Ising ferromagnet.[44] In direct conflict with these contradictory inferences is the result that the exponent δ possesses a value that is in complete disagreement with those predicted by either the $d=3$ Heisenberg model or the $d=3$ Ising model, or even the mean-field model. Moreover, the reported values of critical exponents lead to a *serious violation* of the scaling relations $\alpha+2\beta+\gamma=2$ and $\beta+\gamma=\beta\delta$.

Recently, the high-resolution ''zero-field'' ac susceptibility data taken along the c axis (easy direction of magnetization) of a high-purity Gd single crystal in the reduced temperature range $5.1\times10^{-5}\leqslant\epsilon\leqslant1.2\times10^{-1}$ have demonstrated[42] the following. (i) The asymptotic critical behavior of Gd is that of a *uniaxial dipolar* (UD) ferromagnet in that the susceptibility data are best described by the expression $\chi(\epsilon)\sim|\epsilon|^{-\gamma}|\ln|\epsilon||^{1/3}$ with $\gamma=1$ in the temperature range $5.1\times10^{-5}\leqslant\epsilon\leqslant2.1\times10^{-3}$, which gives the extent of the asymptotic critical region. (ii) As the temperature is raised above T_C, a crossover from UD to the *isotropic dipolar* (ID) fixed point occurs at a sharply defined temperature $\epsilon_{CO}^{UD\rightarrow ID}\simeq2.05(10)\times10^{-3}$ and this crossover, at high temperatures, is followed by a very sluggish ID $\rightarrow$ Gaussian crossover. (iii) The $d=3$ Ising-like values of the susceptibility critical exponent γ reported previously, far from reflecting the true $d=3$ Ising critical behavior, are a manifestation of an extremely slow crossover from ID to Gaussian regime. Encouraged by this development and recognizing that *nonasymptotic* data are at the root[42] of conflicting reports about the nature of leading singularity at T_C in Gd, we undertook a detailed bulk magnetization investigation of the FM-PM phase transition in Gd with a view to resolve the controversy[42] surrounding the nature of its asymptotic critical behavior. To this end, high-resolution magnetization measurements have been performed on the *same* sample of high-purity Gd single crystal as that used previously[42] for ac susceptibility measurements in a temperature range that embraces the critical region. The results of this investigation, combined with those of earlier resistivity,[29] specific heat,[27] and ac susceptibility[42] studies, unambiguously demonstrate that Gd belongs to the $d=3$, $n=1$ *dipolar* universality class.

II. EXPERIMENTAL DETAILS

A detailed description of the growth, purity, and handling of the gadolinium single crystals used in this work is given elsewhere.[42] Extensive high-resolution (relative accuracy better than 50 ppm) magnetization measurements, whose details are furnished below, were performed on the *same* sample as that used previously for ac susceptibility measurements,[42] i.e., on 99.92 at.% pure Gd single crystal of cylindrical shape [1.50(2) mm in diameter and 1.70(2) mm in length], with external magnetic field, H_{ext}, directed along the c axis (which is not only the cylindrical axis but also the easy direction of magnetization). The demagnetizing factor N was computed from the slope of the magnetization, M, versus H_{ext} straight line [i.e., $4\pi N=(\text{slope})^{-1}$] isotherms taken at temperatures well below T_C in the field range -20 Oe$\leqslant H_{ext}\leqslant20$ Oe. The value of $N=0.31(1)$, so obtained, agrees well with that $[N=0.31(1)]$ calculated from the well-known Osborn formula using the actual sample dimensions. Curie temperature, T_C, of the Gd sample in question was estimated by identifying T_C with the temperature at which a *kink* occurs in the thermomagnetic curves recorded at $H_{ext}=10$ and 20 Oe and the value, so obtained, is $T_C=292.8$ K, as shown in the bottom panel of Fig. 1. The bottom panel of Fig. 1 also serves to demonstrate that magnetization *scales* with H_{ext} for $H_{ext}\leqslant20$ Oe. The top panel of Fig. 1 compares the $\chi_{ext}=M/H_{ext}$ data taken at $H_{ext}=10$ Oe with the ac susceptibility data taken previously[42] on the same sample at ac driving field of rms amplitude $H_{ac}=10$ mOe and frequency $\nu=187$ Hz in the presence of a dc field of $H_{dc}=10$ Oe. The agreement between the two sets of susceptibility data is striking and the value of $T_C=292.8$ K obtained by the kink-point method (bottom panel of Fig. 1) conforms very well with that $[T_C=292.77(1)$ K] determined earlier[42] from the ac susceptibility data.

Magnetization, M, versus H_{ext} isotherms in fields up to 15 kOe were measured at *fixed* temperatures $\simeq25$ mK apart in the temperature interval $T_C-4.25$ K$\leqslant T\leqslant T_C+2.2$ K with $T_C=292.8$ K and $\simeq0.1$ K apart over $\simeq8$ K on either side of this temperature region. Each isotherm was obtained by measuring M at 60 predetermined but fixed field values (each stable to within ±0.1 Oe) in the range $0\leqslant H_{ext}\leqslant15$ kOe. The sample temperature was monitored by a precalibrated platinum sensor, which is in body contact (and hence in very good thermal contact) with the sample, and was held constant to within ±5 mK at any setting by means of a proportional, integral, and derivative temperature controller.

III. DATA ANALYSIS AND RESULTS

The ''zero-field'' quantities, such as spontaneous magnetization, $M(T,0)$, and initial susceptibility, $\chi(T)$, have been

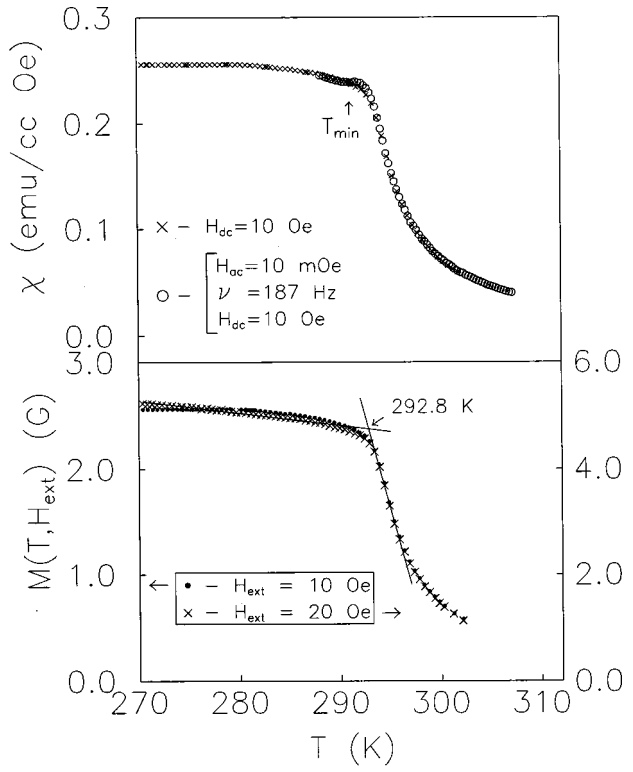

FIG. 1. Temperature dependence of low-field magnetization exhibiting a ''kink'' at $T_C = 292.8$ K and scaling of magnetization with external magnetic field (H_{ext}) in the range 10 Oe$\leqslant H_{ext} \leqslant$20 Oe (bottom panel). A comparison is made between temperature variations of dc and ac susceptibilities at $H_{ext} = 10$ Oe (top panel). Upward arrow marks the temperature at which the minimum in $\chi_{ac}(T)$ occurs.

obtained from the magnetization data taken in finite external magnetic fields at different temperatures by the following extrapolation method. The customary approach[45–48] of using the modified Arrot plot (MAP) to determine T_C and the critical exponents β and γ, when followed, yields the result shown in Fig. 2. It is immediately noticed that the MAP isotherms present substantial deviations from the expected linear behavior particularly at low fields and that the departure from linearity persists to higher fields and becomes more and more pronounced as the temperature takes on values that increasingly deviate from T_C (on either side of T_C). The

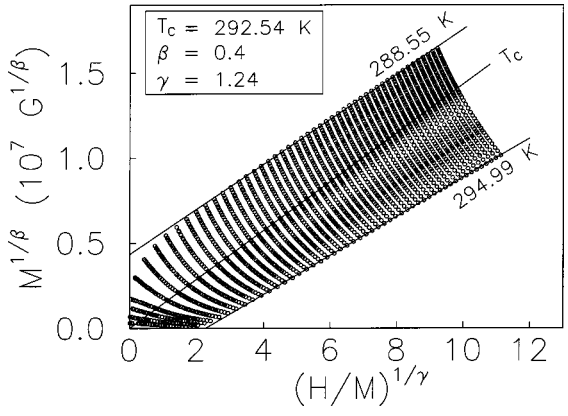

FIG. 2. Modified Arrott plot for temperatures close to T_C.

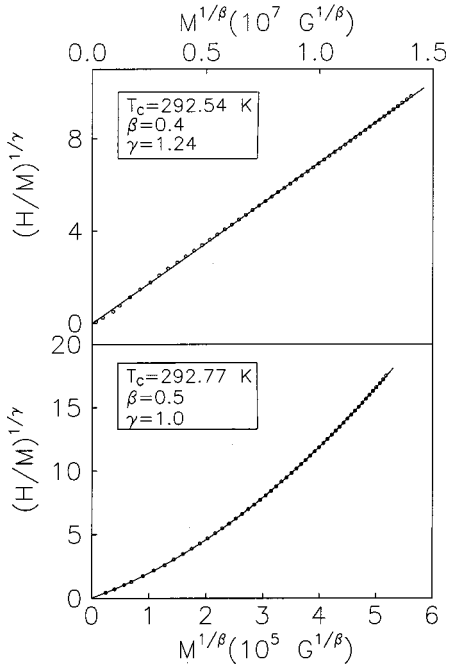

FIG. 3. Critical isotherms and the corresponding best theoretical fits yielded by the scaling equation of state (SES) analysis based on Arrott-Noakes SES (top panel) and mean-field SES [Eq. (1)] (bottom panel).

critical isotherm, when plotted on a sensitive scale (top panel of Fig. 3), reveals that even the optimum choice of β and γ (i.e., $\beta = 0.4$ and $\gamma = 1.24$) does not get rid of its *S*-shaped curvature. Moreover, this approach yields a value ($T_C = 292.54$ K) for T_C which is distinctly different from those obtained from the low-field thermomagnetic curves (Fig. 1) and ac susceptibility data.[42] All of these observations render this extrapolation procedure *unreliable* in the present case.

Next, an attempt has been made to use the *parabolic* extrapolation,[46,47] which is based on the mean-field magnetic equation of state[46]

$$H/M(T,H) = a(T) + b(T)[M(T,H)]^2 + c(T)[M(T,H)]^4. \tag{1}$$

That the *same M* versus *H* isotherms as those used in Fig. 2, when plotted in the form of H/M versus M^2 isotherms, are accurately described by Eq. (1) is evident from the results presented in the bottom panel of Fig. 3, and Fig. 4 wherein the best least-squares fits (depicted by continuous curves), based on Eq. (1), to a few selected H/M versus M^2 isotherms are displayed. These figures clearly demonstrate that (i) this procedure yields exactly the same value (i.e., $T_C = 292.77$ K) for T_C as that obtained previously[42] by an elaborate analysis of the ac susceptibility data, (ii) Eq. (1) reproduces in *facsimile* the observed field dependence of *M* down to the lowest field value of $H \simeq 90$ Oe for temperatures in the range $T_C - 1$ K$\leqslant T \leqslant T_C + 2$ K, and (iii) outside this temperature range, the data start departing from the optimum fits, based on Eq. (1), at low fields, more so for $T < T_C$ than for $T > T_C$, and the field at which such departures first occur increases as the temperature progressively deviates from T_C. For instance, the data depart from the fits at $H \simeq 220$ Oe and 700 Oe for $T = 294.99$ K and 288.55 K,

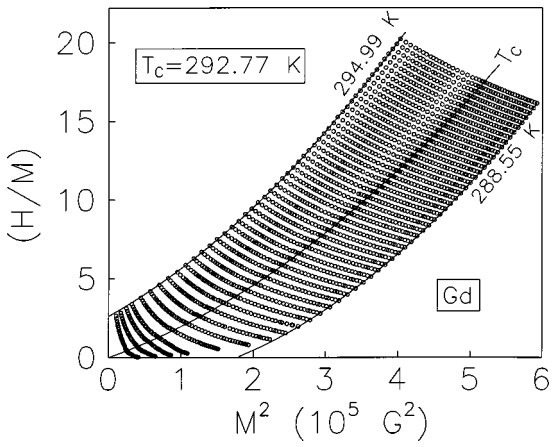

FIG. 4. Data shown in Fig. 2 replotted in the form of (H/M) versus M^2 (Arrott-Belov-Kouvel plot).

respectively, as contrasted with the case of the corresponding MAP isotherms for which the low-field deviations start at $H \simeq 1$ kOe and 3 kOe, respectively. However, in the strict sense, the parabolic extrapolation method too does not lead to sufficiently accurate results for temperatures outside the range $T_C - 2\ \mathrm{K} \lesssim T \lesssim T_C + 2\ \mathrm{K}$ ($T_C = 292.77$ K) especially for temperatures well below T_C. For this reason, the data analysis has been restricted to the temperature range $288.55\ \mathrm{K} \leqslant T \leqslant 294.99\ \mathrm{K}$ only.

A. Spontaneous magnetization

When $H=0$ and $T \leqslant T_C$, Eq. (1) reduces to a quadratic equation in spontaneous magnetization squared, $[M(T,0)]^2 \equiv [M(T,H=0)]^2$, i.e.,

$$c(T)m^2(T) + b(T)m(T) + a(T) = 0, \tag{2}$$

where $m(T) \equiv [M(T,0)]^2$. The values of the coefficients a, b, and c at different temperatures are obtained from the best least-squares fits to the $H/M(T,H)$ versus $[M(T,H)]^2$ isotherms based on Eq. (1). Knowing the values of a, b, and c at a given temperature, spontaneous magnetization at that temperature is computed from the solution of Eq. (2). The temperature dependence of spontaneous magnetization, so obtained, is depicted in Fig. 5. To begin with, $M(T,0)$ data are analyzed in terms of the single power law[31–38,43,46–50] (SPL)

$$M(T,0) = B_{eff} \quad (-\epsilon)^{\beta_{eff}}, \quad \epsilon < 0. \tag{3}$$

The ''range-of-fit'' analysis[46–50] [in which changes in the values of the free fitting parameters, e.g., B_{eff}, T_C^-, and β_{eff} in Eq. (3), and the sum of deviation squares are monitored as the fit range $|\epsilon_{min}| \leqslant \epsilon \leqslant |\epsilon_{max}|$ is varied by keeping $|\epsilon_{min}|(|\epsilon_{max}|)$ fixed at a certain value and varying $|\epsilon_{max}|(|\epsilon_{min}|)$] of the $M(T,0)$ data based on Eq. (3) yields the value for T_C^- as $T_C^- = 292.79(1)$ K. Optimum SPL fit to the $M(T,0)$ data over the entire temperature range $288.55\ \mathrm{K} \leqslant T \lesssim T_C^-$ based on Eq. (3) is represented in Fig. 5 by the continuous curve. The temperature dependence of the *effective* critical exponent β_{eff}, defined as $\beta_{eff}(|\epsilon|) = d[\ln M(|\epsilon|)]/d(\ln|\epsilon|)$, shown in Fig. 6, is then computed from the $M(|\epsilon|)$ data by keeping T_C fixed at the value $T_C^- = 292.78$ K (this choice of T_C^- is justified later). The most

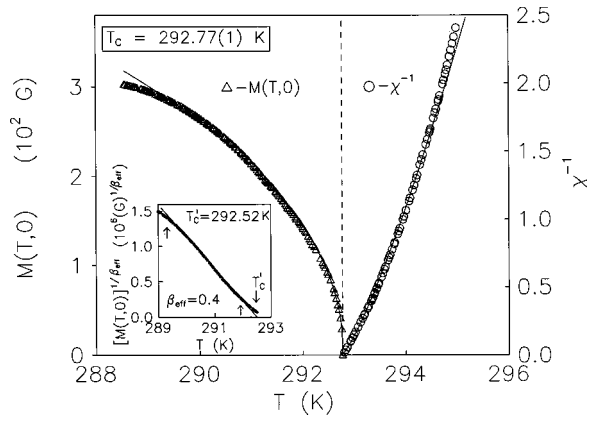

FIG. 5. Temperature variations of spontaneous magnetization, $M(T,0)$, and inverse initial susceptibility, $\chi^{-1}(T)$, in the temperature range that embraces the critical region. The continuous curves through the $M(T,0)$ and $\chi^{-1}(T)$ data are the best least-squares fits based on Eqs. (3) and (5) of the text. The inset shows $[M(T,0)]^{1/\beta_{eff}}$ plotted against T with $\beta_{eff}=0.4$. The straight line through the data represents the best least-squares fit based on Eq. (3) and *upward* arrows indicate the fit range.

striking feature of the $\beta_{eff}(|\epsilon|)$ data presented in Fig. 6 is that β_{eff} possesses values that are very close to the mean-field (MF) value of $\beta = 0.5$ for $|\epsilon| \lesssim 6 \times 10^{-4}$. Suspecting the result $\beta_{eff} \to 0.5$ as $|\epsilon| \to 0$ to be an indication of uniaxial dipolar behavior in the asymptotic critical region (ACR), the relation

$$M(T,0) = \hat{B}(-\epsilon)^{\beta} |\ln|\epsilon||^{x'}, \quad \epsilon < 0, \tag{4}$$

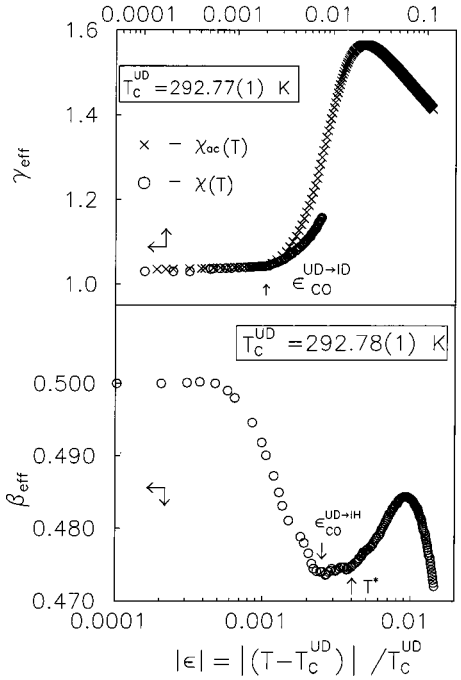

FIG. 6. Temperature variations of the *effective* critical exponents β_{eff} (bottom panel) and γ_{eff} (top panel). Upward arrows in the top and bottom panels indicate the uniaxial dipolar (UD)–to–isotropic dipolar (ID) crossover temperature and the onset temperature of the peak, respectively.

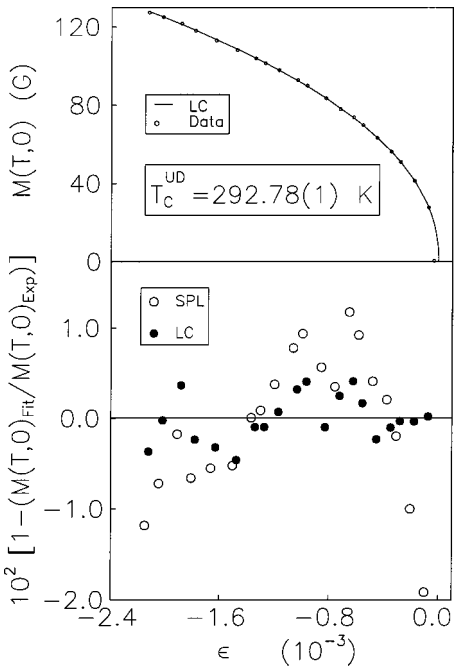

FIG. 7. Spontaneous magnetization, $M(T,0)$, and percentage deviation of $M(T,0)$ data from the best least-squares SPL and LC fits, based on Eqs. (3) and (4) of the text, respectively, as functions of temperature. The continuous curve through the $M(T,0)$ data, denoted by open circles, represents the best least-squares fit based on Eq. (4) of the text.

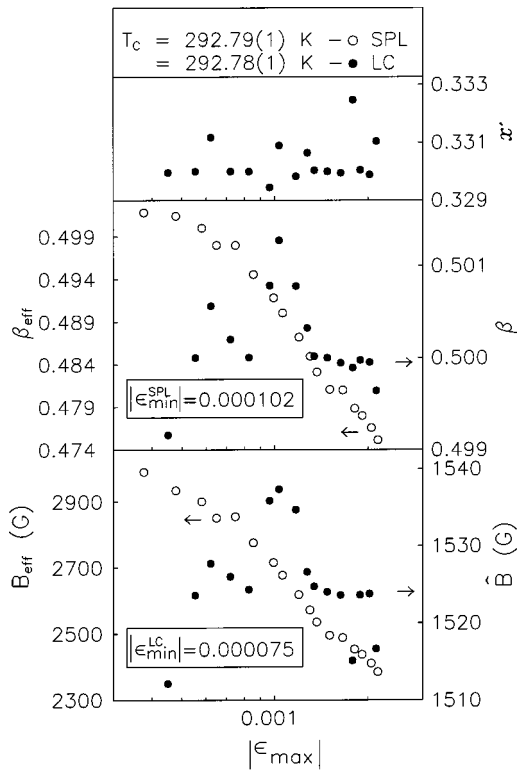

FIG. 8. Variations of the free fitting parameters with $|\epsilon_{max}|$ (see text) in the ''range-of-fit'' analysis of $M(T,0)$ data, using Eqs. (3) and (4) of the text. Note the extreme sensitivity of the ordinate scales for the parameters $\hat{B}$, β, and x'. Left and right arrows indicate the ordinate scales for the data denoted by open and closed circles, respectively.

with $\beta=0.5$, $x'=3/(n+8)$, and $n=1$, predicted[13,16,17,51,52] by the renormalization-group (RG) theories to *leading* order in ϵ for $d=3$ uniaxial dipolar ferromagnets, is used to analyze the $M(T,0)$ data. While fitting the data to Eq. (4), the exponent x' is kept constant at the theoretically predicted[16,17,51,52] value of $x'=1/3$, and $\hat{B}$, T_C^-, and β are treated as free fitting parameters in the first phase of the range-of-fit (ROF) analysis. Having determined the value of T_C^- in this manner, T_C^- is fixed at this value ($T_C^-=292.78$ K), while $\hat{B}$, β, and x' are varied in the second phase of the ROF analysis to optimize agreement between theory and experiment. This approach leads to the optimum fit, based on Eq. (4), to the $M(T,0)$ data in the temperature range $7.5\times10^{-5}\leqslant|\epsilon|\leqslant2.1\times10^{-3}$ (open circles) represented by the continuous curve in Fig. 7. Figure 8 compares the results of the ROF analysis (second phase, with T_C^- fixed) of the spontaneous magnetization data taken in the above-mentioned temperature range based on the single power law (SPL), Eq. (3), and the theoretical expression, Eq. (4), which, besides the single power law, includes the leading multiplicative *logarithmic correction* (LC). Note that the data point taken at a temperature ($T=292.77$ K) closest to T_C has been left out of the analyses based on Eqs. (3) and (4) because its inclusion leads to considerable deterioration in the quality of both SPL and LC fits. From the variations in the values of the parameters T_C^-, $\hat{B}$, β, and x' observed (Fig. 8), while analyzing $M(T,0)$ data in terms of Eq. (4) using the ROF analysis, we arrive at the final result $T_C^-=292.78(1)$ K, $\hat{B}=1526(11)$ G, $\beta=0.5002(6)$, and $x'=0.330(2)$ in the reduced temperature range

$$-2.08(5)\times10^{-3}\leqslant\epsilon\leqslant-7.5\times10^{-5},$$

which gives the extent of the asymptotic critical region (ACR) for $\epsilon<0$.

Other important observations based on the ROF data analysis are as follows. (i) If in the ROF analysis, $|\epsilon_{max}|$ is increased beyond 2.1×10^{-3}, while $|\epsilon_{min}|$ is kept fixed at 7.5×10^{-5}, the quality of LC fits deteriorates very fast, so much so that beyond a certain value of $|\epsilon_{max}|$, Eq. (3) provides better overall (SPL) fit to the data than Eq. (4) (LC fit) does. (B) If only the data outside the ACR are considered in the ROF analysis, SPL fits describe the $M(T,0)$ data better than LC fits and in the temperature range $289.30(5)\leqslant T\leqslant291.90(5)$ K, yield $T_C'=292.52(3)$ K and $\beta_{eff}=0.40(2)$ (inset of Fig. 5). These values of T_C' and β_{eff} are consistent with those yielded by the modified Arrott plot (Fig. 2). $\beta_{eff}=0.40(2)$ is also in consonance with the value $\beta_{eff}=0.399(16)$ yielded earlier[38] by the perturbed angular correlation investigations on Gd in a temperature range similar to the present one.

B. Initial susceptibility

Parabolic extrapolation of the H/M versus M^2 isotherms (Fig. 4) taken at $T\geqslant T_C$ to $M^2=0$ yields intercepts on the ordinate (H/M) axis that directly give the values of inverse initial magnetic susceptibility at different temperatures, i.e., $\chi^{-1}(T)$. It immediately follows from Eq. (1) that $\chi^{-1}(T)=a(T)$. Values of the coefficient a or χ^{-1} at different tem-

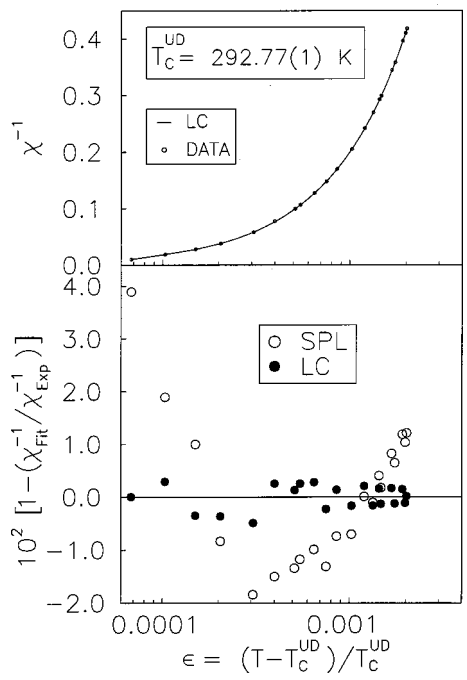

FIG. 9. Inverse initial susceptibility, $\chi^{-1}(T)$, and percentage deviation of the $\chi^{-1}(T)$ data from the best least-squares SPL and LC fits, based on Eqs. (5) and (6) of the text, respectively, as functions of reduced temperature. Continuous curve through the $\chi^{-1}(T)$ data, denoted by open circles, represents the best least-squares fit based on Eq. (6) of the text.

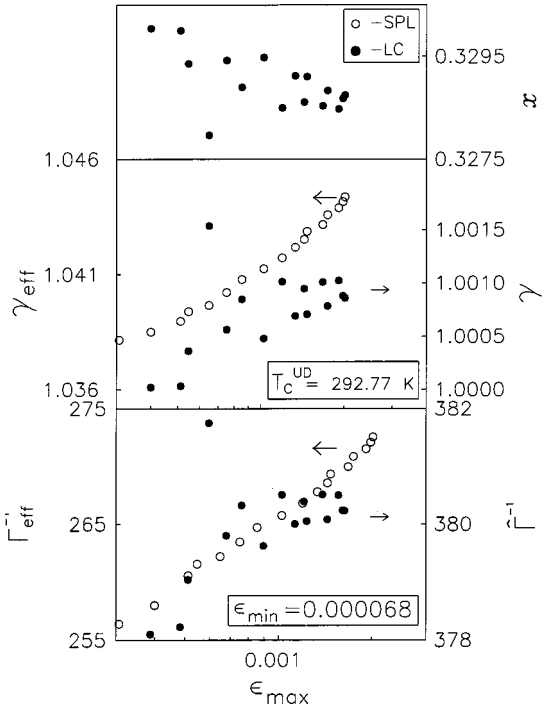

FIG. 10. Variations of the free fitting parameters with ϵ_{max} (see text) in the ''range-of-fit'' analysis of $\chi^{-1}(T)$ data using Eqs. (5) and (6) of the text. Note the extreme sensitivity of the ordinate scales for the parameters $\hat{\Gamma}^{-1}$, γ, and x. Left and right arrows indicate the ordinate scales for the data denoted by open and closed circles, respectively.

peratures $T \geqslant T_C$ obtained from the best least-squares fits to the H/M versus M^2 isotherms based on Eq. (1), are shown in Fig. 5. Like $M(T,0)$ data, $\chi^{-1}(T)$ data are, at first, analyzed in terms of the single power law[31–42,46–50] (SPL),

$$\chi^{-1}(T) = \Gamma_{eff}^{-1} \epsilon^{\gamma_{eff}}, \quad \epsilon > 0. \tag{5}$$

The ''range-of-fit'' analysis[42,46–50] gives $T_C^+ = 292.77$ K for the optimum SPL fit to the $\chi^{-1}(T)$ data in the temperature range $T_C^+ \leqslant T \leqslant 295$ K. Such a fit is denoted by the continuous curve in Fig. 5. Temperature dependence of the *effective* critical exponent γ_{eff}, defined as $\gamma_{eff}(\epsilon) = d[\ln \chi^{-1}(\epsilon)]/d(\ln \epsilon)$, displayed in Fig. 6, is then computed from the $\chi^{-1}(\epsilon)$ data by holding the T_C^+ constant at the above-mentioned value. From the results shown in Fig. 6, it is evident that γ_{eff} attains mean-field-like values (i.e., $\gamma_{eff} \simeq \gamma_{MF} = 1$) for temperatures below a well-defined *crossover* temperature, $\epsilon_{CO} = 2.02(6) \times 10^{-3}$, above which γ_{eff} increases steeply. In Fig. 6, we have compared the $\gamma_{eff}(\epsilon)$ data, deduced from the SPL analysis of the present $\chi^{-1}(\epsilon)$ data (obtained using *parabolic extrapolation*), with that derived from the previous[42] $\chi_{ac}^{-1}(\epsilon)$ data (*directly* measured ac susceptibility in *zero* dc superposed field), using the SPL analysis. An excellent agreement between the two data sets, particularly for $\epsilon \leqslant \epsilon_{CO}$ (i.e., in the asymptotic critical region), is clearly noticed. Now that the observation $\gamma_{eff} \to 1$ as $\epsilon \to 0$ is suggestive of uniaxial dipolar behavior in the asymptotic critical region, the expression

$$\chi^{-1}(T) = \hat{\Gamma}^{-1} \epsilon^{\gamma} |\ln \epsilon|^{-x}, \quad \epsilon > 0, \tag{6}$$

with $\gamma = 1$, $x = (n+2)/(n+8)$, and $n = 1$, yielded by the RG calculations[13,16–19,51,52] to *leading* order in ϵ for the initial susceptibility of $d = 3$ uniaxial dipolar ferromagnets, is used to analyze $\chi^{-1}(T)$ data for $\epsilon \leqslant \epsilon_{CO}$. As already stated in the preceding subsection, the range-of-fit analysis is performed in two phases. In the first phase, the exponent x is kept constant at the theoretically predicted[16–19,51,52] value of $x = 1/3$, and $\hat{\Gamma}^{-1}$, T_C^+, and γ are varied to arrive at the optimum fit. In the second phase, T_C^+ is *fixed* at the value ($T_C^+ = 292.77$ K) obtained in the first phase, while $\hat{\Gamma}^{-1}$, γ, and x are varied so as to arrive at the best fit to the $\chi^{-1}(\epsilon)$ data based on Eq. (6). This fit is depicted by the continuous curve in Fig. 9. A detailed comparison between the results of the analysis (second phase, with T_C^+ fixed) of the $\chi^{-1}(\epsilon)$ data taken in the reduced temperature range $6.8 \times 10^{-5} \leqslant \epsilon \leqslant 2.02 \times 10^{-3}$, based on Eqs. (5) and (6), is made in Fig. 10. Considering the variations in the free fitting parameters observed (Fig. 10) in the ROF analysis based on Eq. (6), we quote the final values for these parameters as $T_C^+ = 292.77(1)$ K, $\hat{\Gamma}^{-1} = 380(2)$, $\gamma = 1.0008(5)$, and $x = 0.329(1)$ in the reduced temperature range $6.8 \times 10^{-5} \leqslant \epsilon \leqslant 2.02(6) \times 10^{-3}$, which gives the width of the asymptotic critical regime (ACR) for $\epsilon > 0$. In a similar temperature range ($5.1 \times 10^{-5} \leqslant \epsilon \leqslant 2.1 \times 10^{-3}$), ROF analysis of the ac susceptibility (χ_{ac}) data taken on the *same* sample as the present one has previously yielded[42] *exactly* the *same* values as quoted above for the parameters T_C^+, γ, and x, but not for $\hat{\Gamma}^{-1}$ for which the present value [380(2)] is roughly 2.96 times larger than the value [128.4(30)] estimated from

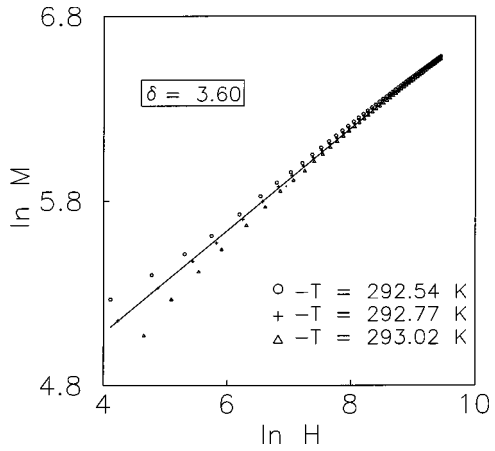

FIG. 11. $\ln M - \ln H$ isotherms at a few selected temperatures around T_C. Note that the isotherm at $T=292.54$ K and $T=292.77$ K are the critical isotherms according to the Arrott-Noakes and mean-field equations of state, respectively.

$\chi^{-1}(T)$. This discrepancy stems from the fact that the $\chi^{-1}(T)$ is *consistently* larger in magnitude than the $\chi_{ac}^{-1}(T)$ by a factor of 2.96, but otherwise their temperature dependences are exactly the same.

For $\epsilon > \epsilon_{CO}$, the above-mentioned analysis reveals that, irrespective of the temperature range chosen, SPL fits [Eq. (5)] describe the $\chi^{-1}(T)$ data better than LC fits [Eq. (6)] and that such a fit in the range $293.6(2)\ \text{K} \leqslant T \leqslant 295\ \text{K}$ yields $\tilde{T}_C = 293.0(2)$ K and $\gamma_{eff} = 1.39(3)$. These values of $\tilde{T}_C$ and γ_{eff} agree quite well with those (T_C^{ID} and γ_{eff}^{ID}) obtained previously[42] from $\chi_{ac}(T)$ data in a similar temperature range.

C. Critical isotherm

The critical exponent δ, which characterizes the $M(T,H)$ versus H isotherm taken at $T=T_C$ (the critical isotherm), is conventionally determined by analyzing the $M-H$ isotherm in the immediate vicinity of T_C in terms of the relation

$$M(T_C,H) = A_0 H^{1/\delta} \tag{7a}$$

or

$$H = D M^{\delta}, \quad \epsilon = 0. \tag{7b}$$

According to Eq. (7a), the plot of $\ln M$ against $\ln H$ at $T=T_C$ should be a straight line with slope δ^{-1} and intercept on the ordinate equal to $\ln A_0$. Such $\ln M - \ln H$ plots, constructed out of the $M-H$ isotherms in close proximity to T_C, displayed in Fig. 11, demonstrate that the $\ln M - \ln H$ isotherm at $T=T_C=292.77$ K alone can be approximated by a straight line over a wide range of H values, whereas the isotherms on either side of T_C exhibit a concave-upward and concave-downward curvature for $T<T_C$ and $T>T_C$, respectively. The curvature becomes more pronounced as the temperature increasingly deviates from T_C. A close scrutiny of the critical isotherm reveals that even the insensitive nature of the log-log scale is unable to conceal the *S*-shaped curvature of the isotherm in question. As a consequence, the value of δ depends on the field range chosen for the fit. For instance, the exponent δ possesses the values 3.60 and 3.75 in the ranges $140\ \text{Oe} \leqslant H \leqslant 12\,600$ Oe and $920 \leqslant H \leqslant 12\,600$ Oe, respectively. Though these numerical estimates fall within the range of reported values of δ, their reliability is in doubt in view of the nonlinear $\ln M - \ln H$ critical isotherm.

The observation[7,8] that the *uniaxial* magnetocrystalline anisotropy constant K_{u_1} as a function of temperature goes through a broad peak at $T \simeq T_C$ and is extremely *sensitive* to the external magnetic field, H_{ext}, while the higher order anisotropy constants are zero in this temperature range, asserts that the field experienced by the spins at $T \simeq T_C$ in Gd is not just $H = H_{ext} - 4\pi N M(T, H_{ext})$ but $H_{eff}(H_{ext}) = H(H_{ext}) + H_K(H_{ext})$, where the uniaxial anisotropy field, $H_K(H_{ext}) = 2K_{u_1}(H_{ext})/M_S$ is a function of H_{ext} and M_S is the saturation magnetization. This consideration prompted us to reanalyze the $M-H$ isotherms in the temperature range $T_C - 0.1\ \text{K} \leqslant T \leqslant T_C + 0.1$ K (with $T_C = 292.77$ K) using the revised version of Eq. (7), in which H is replaced by H_{eff}, and the expression

$$M(T_C,H_{eff}) = \hat{A} H_{eff}^{1/\delta} [(1/\beta\delta)\ln H_{eff}]^{x'} \tag{8a}$$

or

$$H_{eff} = \hat{D} M^{\delta} |\ln|M||^{-3x'}, \quad \epsilon = 0, \tag{8b}$$

with $\delta = 3$, $x' = 3/(n+8)$, and $n=1$, that the RG calculations[13,16–19,51,52] yield for the critical isotherm in $d=3$ uniaxial dipolar ferromagnets. Such a data analysis proceeds as follows. At first, the previously published[8] K'_{u_1} versus H_{ext} data taken at $T=293$ K are least-squares fitted to a polynomial in order to arrive at the values of K'_{u_1} corresponding to the H_{ext} values at which magnetization was measured in the present case. K'_{u_1} values, so obtained, are converted to the anisotropy field $H'_K(H_{ext}) = 2K'_{u_1}(H_{ext})/M_S$ by using the value of magnetization measured at the highest field, i.e., at 15 kOe, for the saturation magnetization M_S. With a view to allow for the deviations, if any, from the functional form of $H'_K(H_{ext})$ at the temperatures of present interest, H_K in the expression for H_{eff} is set equal to $C' H'_K$, where C' (depends on H_{ext}) is a constant if the functional forms of $H'_K(H_{ext})$ and $H_K(H_{ext})$ (do not) match. $M - H_{eff}$ isotherms in the temperature range $292.67 \leqslant T \leqslant 292.87$ K are then least-squares fitted to the revised version of Eq. 7(a), i.e.,

$$M(T_C,H_{eff}) = A'_0 H_{eff}^{1/\delta} \tag{7a'}$$

and Eq. 8(a) by treating A'_0, C', and δ in the former (SPL) fit, and $\hat{A}$, C', and δ in the latter (LC) one, as free fitting parameters. Note that for the fit based on Eq. (8a), the exponents β and x' are kept constant at the values $\beta = 0.5$ and $x' = 0.33$ determined from the spontaneous magnetization data (Sec. III A). Two types of fitting procedures have been adopted. In the first type, the lower limit H_{ext}^{min} of the external field range $H_{ext}^{min} \leqslant H_{ext} \leqslant H_{ext}^{max}$ is kept fixed while H_{ext}^{max} is varied and the alterations in the fitting parameters as functions of H_{ext}^{max} are monitored. This type of ''range-of-fit'' analysis reveals that (i) with the same number of parameters,

Eq. (8a) reproduces the $M(T,H_{eff})$ data far more accurately than Eq. (7a′) does, (ii) $\delta \simeq 2.7$ and 3 for the fits based on Eqs. (7a′) and (8a), respectively, and (iii) a strong correlation exists between δ and C' in both the fits. In the second fitting procedure (the so-called ''sliding-fit-range'' analysis), the range of H_{ext} values used in present measurements is split into several narrow ranges, each containing three successive values of H_{ext}. Starting with the lowest value of H_{ext}, if the $M-H_{eff}$ isotherm data points with increasing $H_{eff}=H_{ext}-4\pi NM+C'(H_{ext})H'_K(H_{ext})$ are labeled by the natural numbers $i=1,2,3,\ldots,n$, the first fit range covers the data points 1,2,3, the second one 2,3,4, and so on. For LC (SPL) fits in these ranges δ is set equal to 3 (2.7), while $\hat{A}$ and C' (A'_0 and C') are varied to optimize agreement between theory and experiment. This method brings out clearly the actual functional form of $C'(H_{ext})$ since $H'_K(H_{ext})$ is known (see the foregoing text). To elucidate this point further, now that the H_{ext} values are equally spaced, the value of C' obtained in a given range, which spans the values H_{ext}^{n-2}, H_{ext}^{n-1}, and H_{ext}^{n}, corresponds to the middle value H_{ext}^{n-1} of the range. The main outcome of this exercise is that C' depends on H_{ext}. This observation implies that the functional form of $H_K(H_{ext})$ differs from that of $H'_K(H_{ext})$ by as much as $C'(H_{ext})$. In order to get rid of the field dependence of C' and hence ensure that $H_K(H_{ext})=\text{const}\times H'_K(H_{ext})$, the functional form of $H'_K(H_{ext})$ is slightly modified and the above fitting procedures repeated to first arrive at the *optimum* value of δ and then calculate $C'(H_{ext})$ corresponding to this value of δ. Such an *iterative* method determines the exponent δ, the amplitude $\hat{A}$ or A'_0 and $H_K(H_{ext})$ [and hence $H_{eff}(H_{ext})$] *self-consistently*. Figure 12 displays the $M-H_{ext}$ isotherm at $T=T_C=292.77$ K, obtained in this way, in the form of (H_{eff}/M) versus M^2 plot while the inset shows the variation of K_{u_1} with H_{ext} at $T=292.77$ K that the iterative process finally yields and compares it with the observed[8] field dependence of K_{u_1} at $T=293$ K. For a temperature which is lower than 293 K, the presently determined variation of K_{u_1} with H_{ext} is consistent with the field variations of K_{u_1} at different temperatures displayed in Fig. 2 of Ref. 8. The continuous curve through the $(H_{eff}/M)-M^2$ data points in Fig. 12 represents the best theoretical (LC) fit based on Eq. (8a). This fit is far superior in quality to that (SPL) based on Eq. (7a′), as is evident from the fact that, according to Eq. (7a′), (H_{eff}/M) versus M^2 plot at $T=T_C$ should be a straight line passing through the origin. With a conservative estimate of errors, the present data analyses of the isotherms in the immediate vicinity of T_C yields the final values for the quantities of interest as $T_C=292.77(1)$ K, $\hat{A}=17.5(15)$, and $\delta=3.005(5)$.

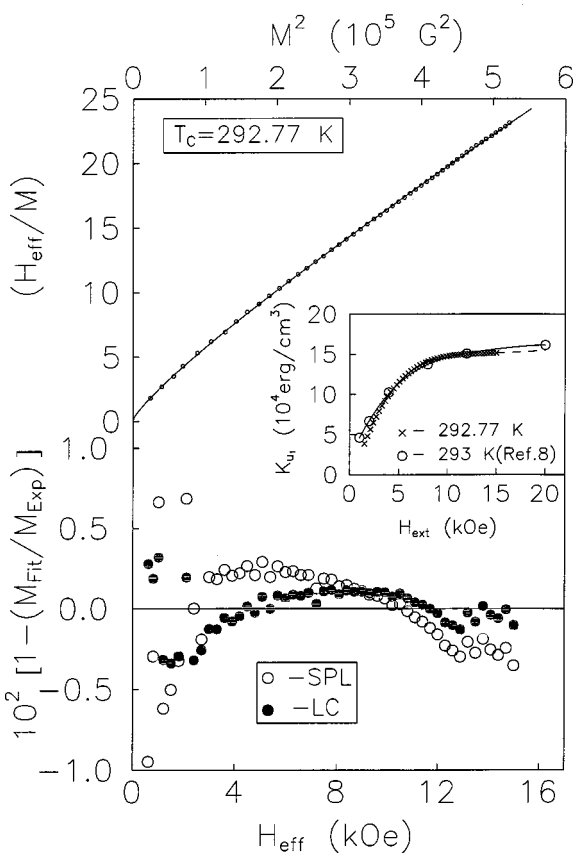

FIG. 12. $(H_{eff}/M)-M^2$ isotherm at $T=T_C=292.77$ K. The continuous curve through the $(H_{eff}/M)-M^2$ data points, denoted by closed circles, represent the best least-squares fit based on Eq. (8a) of the text. Percentage deviations of the $M(T_C,H_{eff})$ data from the best least-squares SPL and LC fits, based on Eqs. (7a′) and (8a) of the text, respectively, as a function of effective field H_{eff}. The inset compares the variations with the external magnetic field H_{ext} of the uniaxial anisotropy constant K_{u_1} at $T=293$ K (open circles), reported in Ref. 8, and $T=292.77$ K (crosses), arrived at by the self-consistent iteration method (see text).

IV. DISCUSSION

From the results of the ''range-of-fit'' analysis of the spontaneous magnetization, $M(T,0)$, and inverse initial susceptibility, $\chi^{-1}(T)$, in the asymptotic critical region, in terms of Eqs. (3)–(6) presented in Figs. 8 and 10, the following observations can be made. (i) While the *effective* amplitude B_{eff} $[\Gamma_{eff}^{-1}]$ and *effective* critical exponent β_{eff} $[\gamma_{eff}]$ appearing in Eq. (3) [Eq. (5)] constantly *decreases* [*increases*] with $|\epsilon_{max}|$, *asymptotic* amplitude $\hat{B}$ $[\hat{\Gamma}^{-1}]$, *asymptotic* critical exponent β $[\gamma]$ and the exponent x' $[x]$ of the logarithmic correction, defined by Eq. (4) [Eq. (6)], *do not depend* (within the uncertainty limits) on $|\epsilon_{max}|$. (ii) Barring the *nonuniversal* critical amplitude $\hat{B}$ $[\hat{\Gamma}^{-1}]$, the exponents β $[\gamma]$ and x' $[x]$ possess the *same* (within the error bars) values as those $\beta=0.5$ $[\gamma=1.0]$ and $x'=3/(n+8)$ $[x=(n+2)/(n+8)]$ predicted[13,16–19,51,52] by the renormalization group (RG) theories for $d=3$, $n=1$ (*uniaxial*) *dipolar* ferromagnet. The above observations (i) and (ii) not only clearly bring out the importance of the multiplicative logarithmic correction but also assert that the asymptotic critical behavior of gadolinium is that of a $d=3$ *uniaxial dipolar* (UD) ferromagnet or, alternatively, that Gd belongs to the $d=3$, $n=1$ dipolar static universality class. This claim is further substantiated by the finding (bottom panel of Figs. 7, 9, and 12) that in the entire asymptotic critical region $-2.1\times10^{-3}\leqslant\epsilon\leqslant2.0\times10^{-3}$, including $\epsilon=0$, the *percentage deviation* of the $M(T,0)$, $\chi^{-1}(T)$, and $M(T_C,H_{eff})$ data from the best least-squares LC fits, based on Eqs. (4),

(6), and (8a), respectively, does not exceed ± 0.5 and is *evenly* distributed around the theoretically calculated values, whereas the optimum SPL fits, based on Eqs. (3), (5), and (7a′), respectively, present *systematic* deviations from the data in question that are as large as $\pm 2\%$. The Curie temperature values T_C^-, T_C^+, and T_C that the data analyses based on Eqs. (4), (6) and (8a) yield are the *same* (within error limits) and equal the Curie temperature for the uniaxial dipolar fixed point, i.e., $T_C^- = T_C^+ = T_C \equiv T_C^{UD}$. Moreover, the presently determined values of the *asymptotic* critical exponents β, γ and δ, along with the previously reported[27,29] value $\alpha^{\pm} = 0$ of the specific heat critical exponent, obey the scaling relations $\beta + \gamma = \beta\delta$ and $\alpha + 2\beta + \gamma = 2$ to an extremely high degree of accuracy. Now that the LC fits are far superior in quality to SPL fits and yield more accurate value for T_C, T_C^- is kept fixed at $T_C^- = 292.78$ K for computing $\beta_{eff}(\epsilon)$ (Fig. 6).

Considering the well-known[46,47,47–53] fact that the critical exponents by themselves do not fully characterize the asymptotic critical behavior but do so only in association with the corresponding critical amplitudes and that the asymptotic critical amplitude *ratios*, like asymptotic critical exponents, are *universal*, conclusive evidence for the $d=3$ uniaxial dipolar asymptotic critical behavior of Gd can be provided only when the universal amplitude ratio $R_\chi = \hat{D}\hat{B}^{\delta-1}\hat{\Gamma} = (\hat{A}/\beta^{x'})^{-\delta}\ \hat{B}^{\delta-1}/\hat{\Gamma}^{-1}$, where the critical amplitudes $\hat{B}$, $\hat{\Gamma}^{-1}$, $\hat{A}$, or $\hat{D}$ are defined by the Eqs. (4), (6), (8a), or (8b), like the critical exponents α, β, γ, and δ, possesses the value that is theoretically predicted[51–53] for a system belonging to the $d=3$, $n=1$ dipolar universality class. From the values of the quantities $\hat{A}$, β, x', δ, $\hat{B}$, and $\hat{\Gamma}^{-1}$ determined in this work (Sec. III), we obtain the value $R_\chi = 0.58(12)$. This value should be compared with the numerical estimates[46,51–53] 1.33(1), 1.6(1), 1.0, and 0.5 given for this ratio by the RG calculations in the case of $d=3$ Heisenberg, $d=3$ Ising, $d=3$ Mean-field, and $d=3$, $n=1$ dipolar spin systems. The finding that the value $R_\chi = 0.58(12)$, determined in this work, conforms well with $R_\chi = 0.5$, expected for a $d=3$, $n=1$ dipolar ferromagnet, but not with the mean-field value $R_\chi = 1.0$ provides not only a direct experimental proof for the existence of logarithmic corrections at an upper marginal space dimension of $d^*=3$ for dipolar Ising spin system but also a *clinching* evidence for the $d=3$ *uniaxial dipolar* asymptotic critical behavior of Gd. This conclusion is consistent with the inference recently drawn[54] from the existing data on critical spin dynamics in Gd.

A close agreement between $\chi^{-1}(T)$ and $\chi_{ac}^{-1}(T)$ for temperatures within and outside ACR, when viewed in the light of arguments presented by us previously,[42] asserts that a crossover from *uniaxial dipolar* (UD) to *Isotropic dipolar* (ID) critical behavior occurs at a well-defined temperature $\epsilon_{CO}^{UD\to ID} = 2.02(6)\times 10^{-3}$ as the temperature is raised above T_C^{UD}. Moreover, $\epsilon_{CO}^{UD\to ID}$ matches $\epsilon_{CO}^{ID\to UD}$ [the crossover temperature referred to $T_C^{ID} \equiv \tilde{T}_C = 293.0(2)$ K] $= [293.6(2) - T_C^{ID}]/T_C^{ID} = 2.05(15)\times 10^{-3}$. By contrast, the lowering of temperature below T_C^{UD} results in a crossover from UD to *isotropic* short-range Heisenberg (IH) fixed point at a temperature $\epsilon_{CO}^{UD\to IH} = -2.08(5)\times 10^{-3}$, which should be compared with $\epsilon_{CO}^{IH\to UD}$ [the crossover temperature referred to $T_C^{IH} \equiv T_C' = 292.52(3)$ K] $= [291.90(5) - T_C^{IH}]/T_C^{IH} = -2.1(1)\times 10^{-3}$. It is immediately noticed that $\epsilon_{CO}^{UD\to IH} = \epsilon_{CO}^{IH\to UD}$ (within the uncertainity limits). Though the value $\beta_{eff} = 0.40(2)$ spans the predictions of both $d=3$ isotropic short-range (ISR) Heisenberg model and the model for $d=n=3$ ferromagnets with ID interactions, we contend that the presently determined value of β_{eff} characterizes the $d=3$ ISR Heisenberg fixed point on the grounds that T_C^{IH} does not equal T_C^{ID} but is shifted to lower temperatures with respect to it.

Another important feature of the present results is that for temperatures below T_C, ac susceptibility, $\chi_{ac}(T)$, as a function of temperature goes through a broad minimum at a temperature T_{min} (Fig. 1) where the *effective* critical exponent for spontaneous magnetization $\beta_{eff}(T)$ starts increasing after going through a minimum (T^* in Fig. 6), i.e., $T_{min} = T^* = 291.3(3)$ K. The single power law fit to the $M(T,0)$ data based on Eq. (3) and shown in the inset of Fig. 5 also starts deviating from the data at a temperature $T = 291.9$ K, which is very close. A similar dip in $\chi_{ac}(T)$ at $T_{min} = 291.5$ K has also been observed previously by Aliev *et al.*[36] but with no corresponding structure in either $\beta_{eff}(T)$ or $M(T,0)$. These authors were first to recognize that this dip in $\chi_{ac}(T)$ at a temperature just below T_C is a manifestation of a transition from the Bloch domain wall to linear domain wall. Such a transition is expected[55] to occur in magnetic materials such as Gd (in which uniaxial magnetocrystalline anisotropy does not vanish even for temperatures in the immediate vicinity of T_C) at a temperature below T_C where the condition[55] $M^2(T,0)/8\chi_p = K_{u_1}$ (χ_p is the paraprocess susceptibility) is satisfied. Assuming that both $M(T,0)$ and χ_p follow a power law behavior at such temperatures (Fig. 5), i.e., $M(T,0) = B_{eff}(-\epsilon)^{\beta_{eff}}$ and $\chi_p = (\Gamma_{eff}/2)(-\epsilon)^{-\gamma_{eff}}$ (in arriving at the latter expression, the validity of relations $\Gamma_{eff}/\Gamma'_{eff} = 2$ and $\gamma'_{eff} = \gamma_{eff}$ has been assumed), a crude estimate of the temperature T^{**} at which a transition from Bloch to linear domain wall occurs, according to the above condition,[55] can be obtained from the expression

$$T^{**} = T_C[1 - (4\Gamma_{eff}K_{u_1}/B_{eff}^2)^{1/(2\beta_{eff}+\gamma_{eff})}]. \qquad (9)$$

Inserting the values $B_{eff} = 2318(20)$ G, $\beta_{eff} = 0.469(4)$, $\Gamma_{eff} = 3.78(12)\times 10^{-3}$, $\gamma_{eff} = 1.040(4)$, $T_C = 292.78(1)$ K, and $K_{u_1} = 4.6\times 10^4$ erg/c.c (Ref. 8) in Eq. (9), yields $T^{**} = 290(1)$ K, a value which is in reasonable agreement with the observed value of T_{min} and T^*. The theory[55] that yields the above condition also predicts that the change in $M(T,0)$ across the Bloch-to-linear domain wall transition does not exceed 1%. That such a small change in magnetization could be detected with ease in the present experiments supports our claim that a very high relative accuracy has been achieved in the magnetization measurements. Note that such a domain wall transition is not abrupt but occurs gradually. The close proximity of the Bloch (Heisenberg) domain wall-to-linear (uniaxial dipolar/Ising) domain wall transition temperature $T_{min} = T^* = 291.3(3)$ K to the temperature $T_{CO}^{IH\to UD} = 291.90(5)$ K, at which a crossover from $d=3$

ISR Heisenberg to $d=3$ uniaxial dipolar critical behavior occurs, supports our earlier contention about the nature of crossover at $\epsilon_{CO}^{IH\rightarrow UD}$.

V. SUMMARY

This paper reports the results of detailed bulk magnetization measurements performed in the critical region near the ferromagnetic-to-paramagnetic phase transition on high-purity gadolinium single crystal sample along the c axis (which is the easy direction of magnetization in the present case) and compares them with those of the ''c axis'' ac susceptibility measurements[42] taken on the *same* sample by us previously. Closer approach to T_C by *two decades* in reduced temperature $\epsilon=(T-T_C)/T_C$ than in previous investigations, facilitated mainly by lower impurity levels in the gadolinium single crystal used in the present magnetization and previous[42] ac susceptibility experiments, considerably higher (better than 50 ppm) precision achieved in such measurements and elaborate data analyses have not only permitted an unambiguous detection of the slowly varying logarithmic corrections but also an accurate determination of their exponents x', x and the critical exponents β, γ, and δ that characterize the asymptotic critical behavior of Gd. The finding that the values of the critical exponents β, γ, δ, the exponents of the logarithmic corrections and the universal amplitude ratio $R_\chi=\hat{D}\hat{B}^{\delta-1}\hat{\Gamma}$ are in perfect agreement with those predicted by the renormalization group calculations for $d=3$ dipolar Ising spin system, permits us to conclude that the critical behavior of Gd is that of a three-dimensional *uniaxial dipolar* ferromagnet. Hence the present investigation resolves the long-standing puzzle about the universality class to which Gd belongs by providing conclusive experimental evidence for the $d=3$, $n=1$ dipolar universality class for Gd. Moreover, the presently determined values of the critical exponents β, γ, and δ, along with the previously reported value $\alpha^{\pm}=0$ of the specific heat critical exponent, obey the scaling relations $\beta+\gamma=\beta\delta$ and $\alpha+2\beta+\gamma=2$ (that were seriously violated by the previously published values of α, β, γ, and δ) to an extremely high degree of accuracy. Additional observations include a crossover from uniaxial dipolar to isotropic short-range Heisenberg critical behavior which occurs at $\epsilon_{CO}^{UD\rightarrow IH}=-2.08(5)\times10^{-3}$ and is accompained by a transition from linear (uniaxial dipolar/Ising) domain wall to Bloch (Heisenberg) domain wall as the temperature is lowered below T_C^-.

*Author to whom correspondence should be addressed. Electronic address: kaulsp@uohyd.ernet.in

[1] H. E. Nigh, S. Legvold, and F. H. Spedding, Phys. Rev. **132**, 1092 (1963).

[2] K. P. Belov, Yu. V. Ergin, R. Z. Levitin, and A. V. Ped'ko, Zh. Éksp. Tesr. Fiz. **47**, 2080 (1964) [Sov. Phys. JETP **20**, 1397 (1965)].

[3] F. Milstein and L. B. Robinson, Phys. Rev. **177**, 904 (1969).

[4] G. Will, R. Nathans, and H. A. Alperin, J. Appl. Phys. **35**, 1045 (1964).

[5] J. W. Cable and E. O. Wollan, Phys. Rev. **165**, 733 (1968).

[6] H. R. Child, Phys. Rev. B **18**, 1247 (1978).

[7] W. D. Corner, W. C. Roe, and K. N. R. Taylor, Proc. Phys. Soc. London **80**, 927 (1962).

[8] C. D. Graham, Jr., J. Appl. Phys. **34**, 1341 (1963).

[9] W. D. Corner and B. K. Tanner, J. Phys. C **9**, 627 (1976).

[10] N. M. Fujiki, K. De'Bell, and D. J. W. Geldart, Phys. Rev. B **36**, 8512 (1987).

[11] D. J. W. Geldart, P. Hargraves, N. M. Fujiki, and R. A. Dunlap, Phys. Rev. Lett. **62**, 2728 (1989).

[12] R. A. Dunlap, N. M. Fujiki, P. Hargraves, and D. J. W. Geldart, J. Appl. Phys. **76**, 6338 (1994).

[13] A. Aharony, Phys. Rev. B **8**, 3363 (1973); A. D. Bruce and A. Aharony, *ibid.* **10**, 2078 (1974).

[14] A. D. Bruce, J. M. Kosterlitz, and D. R. Nelson, J. Phys. C **9**, 825 (1976); T. Nattermann and S. Trimper, *ibid.* **9**, 2589 (1976).

[15] A. D. Bruce, J. Phys. C **10**, 419 (197); E. Frey and F. Schwabl, Phys. Rev. B **43**, 833 (1991).

[16] A. I. Larkin and D. E. Khmel'nitskii, Zh. Éksp. Teor. Fiz. **56**, 2087 (1969) [Sov. Phys. JETP **29**, 1123 (1969)]; F. J. Wegner and E. K. Riedel, Phys. Rev. B **7**, 248 (1973).

[17] E. Brézin and J. Zinn-Justin, Phys. Rev. B **13**, 251 (1976).

[18] E. Frey and F. Schwabl, Phys. Rev. B **42**, 8261 (1990).

[19] K. Ried, Y. Millev, M. Fähnle, and H. Kronmüller, Phys. Rev. B **51**, 15 229 (1995), and references cited therein.

[20] J. Kötzler and W. Scheithe, Solid State Commun. **12**, 643 (1973); J. Kötzler and G. Eiselt, Phys. Lett. **58A**, 69 (1976).

[21] G. Ahlers, A. Kornblit, and H. J. Guggenheim, Phys. Rev. Lett. **34**, 1227 (1975); J. Als-Nielsen, *ibid.* **37**, 1161 (1976); J. A. Griffin, J. C. Litster, and A. Linz, *ibid.* **38**, 251 (1977); P. Beanvillain, C. Chappert, and L. Laursen, J. Phys. C **13**, 1481 (1980).

[22] R. Frowein and J. Kötzler, Z. Phys. B **25**, 279 (1976); R. Frowein, J. Kötzler, and W. Assmus, Phys. Rev. Lett. **42**, 739 (1979); R. Frowein J. Kotzler, B. Schaub, and H. G. Schuster, Phys. Rev. B **25**, 4905 (1982).

[23] J. Brinkmann, R. Courths, and H. J. Guggenheim, Phys. Rev. Lett. **40**, 1286 (1978).

[24] E. A. S. Lewis, Phys. Rev. B **1**, 4368 (1970).

[25] D. S. Simons and M. B. Salamon, Phys. Rev. B **10**, 4680 (1974).

[26] P. C. Lanchester, K. Robinson, D. P. Baker, I. S. Williams, R. Street, and E. S. R. Gopal, J. Magn. Magn. Mater. **15-18**, 461 (1980); K. Robinson and P. C. Lanchester, Phys. Lett. **A64**, 467 (1978).

[27] G. Bednarz, D. J. W. Geldart, and M. A. White, Phys. Rev. B **47**, 14 247 (1993).

[28] D. A. Dolejsi and C. A. Swenson, Phys. Rev. B **24**, 6326 (1981).

[29] D. J. W. Geldart, K. De'Bell, J. Cook, and M. J. Laubitz, Phys. Rev. B **35**, 8876 (1987).

[30] C. D. Graham, Jr., J. Appl. Phys. **36**, 1135 (1965).

[31] P. Heller, Rep. Prog. Phys. **30**, 731 (1967).

[32] M. Vincentini-Missoni, R. I. Joseph, M. S. Green, and J. M. H. Levelt Sengers, Phys. Rev. B **1**, 2312 (1970).

[33] M. N. Deschizeaux and G. Develey, J. Phys. (Paris) **32**, 319 (1971).

[34] A. G. A. M. Saleh and N. H. Saunders, J. Magn. Magn. Mater. **29**, 197 (1982).

[35] P. Molho and J. L. Porteseil, J. Phys. (Paris) **44**, 871 (1983).

[36] Kh. K. Aliev, I. K. Kamilov, and A. M. Omarov, Zh. Éksp. Teor. Fiz. **94**, 153 (1988) [Sov. Phys. JETP **67**, 2262 (1988)].

[37] M. Seeger, Ph.D. thesis, Stuttgart University, Germany, 1991 (unpublished).

[38] A. R. Chowdhury, G. S. Collins, and C. Hohenemser, Phys. Rev. B **33**, 6231 (1986).
[39] G. H. J. Wantenaar, S. J. Campbell, D. H. Chaplin, T. J. Mckenna, and G. V. H. Wilson, J. Phys. C **13**, L863 (1980); Phys. Rev. B **29**, 1419 (1984).
[40] P. Hargraves, R. A. Dunlap, D. J. W. Geldart, and S. P. Ritcey, Phys. Rev. B **38**, 2862 (1988).
[41] U. Stetter, M. Farle, K. Baberschke, and W. G. Clark, Phys. Rev. B **45**, 503 (1992).
[42] S. Srinath, S. N. Kaul, and H. Kronmüller, Phys. Rev. B **59**, 1145 (1999).
[43] A.R. Chowdhury, G.S. Collins, and C. Hohenemser, Phys. Rev. B **30**, 6277 (1984).
[44] J. C. Le Guillou and J. Zinn-Justin, Phys. Rev. B **21**, 3976 (1980).
[45] A. Arrott and J. E. Noakes, Phys. Rev. Lett. **19**, 786 (1967).
[46] S. N. Kaul, J. Magn. Magn. Mater. **53**, 5 (1985).
[47] S. N. Kaul and M. Sambasiva Rao, J. Phys.: Condens. Matter **6**, 7403 (1994) M. Sambasiva Rao and S.N. Kaul, J. Magn. Magn. Mater. **147**, 149 (1995).
[48] P. D. Babu and S. N. Kaul, J. Phys.: Condens. Matter **9**, 7189 (1997).
[49] S. N. Kaul, Phys. Rev. B **38**, 9178 (1988); S. N. Kaul and M. Sambasiva Rao, *ibid.* **43**, 11 240 (1991).
[50] S. N. Kaul and Ch. V. Mohan, Phys. Rev. B **50**, 6157 (1994); M. Seeger, S. N. Kaul, H. Kronmüller, and R. Reisser, *ibid.* **51**, 12 585 (1995).
[51] E. Brezín, J. Phys. (Paris) **36**, L-51 (1975).
[52] A. Aharony and P. C. Hohenberg, Phys. Rev. B **13**, 3081 (1976).
[53] V. Privman, P. C. Hohenberg, and A. Aharony, *Phase Transitions and Critical Phenomena*, edited by C. Domb and J. L. Lebowitz (Academic, New York, 1991), p. 1.
[54] E. Frey, F. Schwabl, S. Henneberger, O. Hartmann, R. Wäppling, A. Kratzer, and G. M. Kalvius, Phys. Rev. Lett. **79**, 5142 (1997), and references cited therein.
[55] A. Hubert, in *Lecture Notes in Physics*, edited by J. Ehlers, K. Hepp, and H. A. Weidenmüller (Springer, Berlin, 1974), Vol. 26.